

## THE EXAMINATION OF SURFACE ROUGHNESS PARAMETERS IN THE FINE TURNING OF HYPEREUTECTIC ALUMINIUM ALLOYS

Richárd HORVÁTH<sup>1</sup>, Ágota DRÉGELYI-KISS<sup>2</sup>, Gyula MÁTYÁSI<sup>3</sup>

*Precise knowledge of the machinability of aluminium is more and more important nowadays because aluminium alloys are used by many industries (e.g. the automotive, aerospace and defence industries) and therefore their importance is growing. Two of the most common indices of surface quality are  $R_a$  (average surface roughness) and  $R_z$  (surface height). However, these surface roughness parameters generally used in the industry do not properly characterise the expected behaviour of machined surfaces in operating conditions. The statistical parameters of surface roughness  $R_{sk}$  (skewness) and  $R_{ku}$  (kurtosis) are more suitable to describe it. In this article the machinability of hypereutectic aluminium alloy (with silicon) parts was examined with the help of design of experiments (DOE). The examinations were carried out with different edge geometry diamond tools. The general and statistical values of machined surface roughness were analysed in detail. Conclusions were drawn on the effect of the geometry of the tools used on surface roughness.*

**Keywords:** design of experiment, surface roughness, topological map, aluminium fine-turning

### 1. Introduction

The measurement and evaluation of the surface roughness of machined parts is a widely used method in industry [1, 2]. Determining and examining the surface roughness of workpieces machined with different methods is an important field of research nowadays. Miko et al. used an end-ball milling tool and examined expected surface roughness [3]. His conclusion was that the relationship between the normal vector of the surface and the vector of the tool axis influenced surface roughness. Surface roughness was examined in the case of traditional and so-called rotation turning by Sztankovics and Kundrák [4]. Surface roughness in

<sup>1</sup> Assistant lecturer, Bánki Donát Faculty of Mechanical and Safety Engineering, Óbuda University, 8 Nepszínház street, Budapest, Hungary, e-mail: horvath.richard@btk.uni-obuda.hu

<sup>2</sup> Associate professor, Bánki Donát Faculty of Mechanical and Safety Engineering, Óbuda University, 8 Nepszínház street, Budapest, Hungary, e-mail: dregelyi.agota@btk.uni-obuda.hu

<sup>3</sup> Associate professor, Budapest University of Technology and Economics, 1 Egry J. street, Budapest, Hungary, Romania, e-mail: matyasi@manuf.bme.hu

the case of face milling was determined by Felhő and Kundrák, where the theoretical and the measurement values showed a good fit [5]. The approximation was better when an octagonal insert was used than when a circular insert was used. Dabnum examined the machinability of a special glass-ceramic material by uncoated tools under dry cutting conditions. An equation depending on input parameters was built up to estimate of the metal removal rate and  $Ra$  [6]. Mankova et al. examined the chip deformation of coated and uncoated drills with the Taguchi method and built a mathematical model with the machining parameters as input [7].

Cutting time has an impact on surface roughness and the capability of the cutting to produce surface roughness. In this respect, Kundrák and Pálmai's statement is remarkable [8]: 'in a wider technological range, the function  $T=f(vc)$  has extreme values as well, which can be described by the general tool-life function. The general tool-life equation can be defined even under manufacturing conditions. In terms of cutting time, a turning experiment of MMC with a PCD tool was carried out by Davim [9]. An empirical model was created to estimate  $Ra$ . The model included all the cutting time of the tool (along with the cutting parameters) therefore the changing of surface roughness due to tool wear can also be calculated. Aouici machined hard steel (AISI H11) with a CBN tool. In his work he built a model for the estimation of  $Ra$ , in which the hardness of the workpiece was also considered [10]. When designing surface roughness, the grooving of the surface can be calculated using the geometries of the workpiece and the tool, and their relative movement. Tukora and Szalai showed an example of such a calculation in real time using the parallel processors of a GPU [11]. So-called softcomputing techniques [12, 13] utilize experience gathered concerning surface roughness, and factors influencing it. The authors have published several articles on the machinability of aluminium alloys. They created phenomenological models for the estimation of the parameters  $Ra$  and  $Rz$  [14], and used desirability functions [15, 16] and a numerical method [17] to find the optimum point where productivity was maximum and surface roughness was minimum.

The statistical index numbers of machined surface roughness are defined by the so-called topological map [18] (Fig. 1). It can be seen in Fig. 1. that the  $Rsk$  and  $Rku$  values (their definition can be found in chapter 2.3.) of the surfaces made with different cutting technologies make up groups depending on the cutting technologies used. The difference between these groups explains why surfaces made with different technologies behave differently during operation.

The tribological behaviour of technological surfaces are related to the micro-geometry of surfaces [19]. Several studies have revealed connections between the working properties of surfaces, and  $Rsk$  and  $Rku$  parameters. AISI 5140 steel was turned with ISO and Wiper ceramic tools by Grzesik and Zak. After machining, the surfaces were superfinished and ball burnished. It was

observed that surfaces with better wear resistance had negative  $R_{sk}$  and high  $R_{ku}$  values [20]. Sedlacek investigated the relationship between wear, friction and the statistical parameters of surface roughness. Friction was the smallest in those places where  $R_{ku}$  was the highest and the value of  $R_{sk}$  was the lowest [21]. Pradeep abraded aluminium of high purity. He stated a negative correlation between  $R_{ku}$  and friction as well as a weak positive correlation between  $R_{sk}$  and friction [22]. Barányi examined the connection between the surface roughness parameters  $R_{sk}$  and  $R_{ku}$  in the course of an abrasive wear process [23].

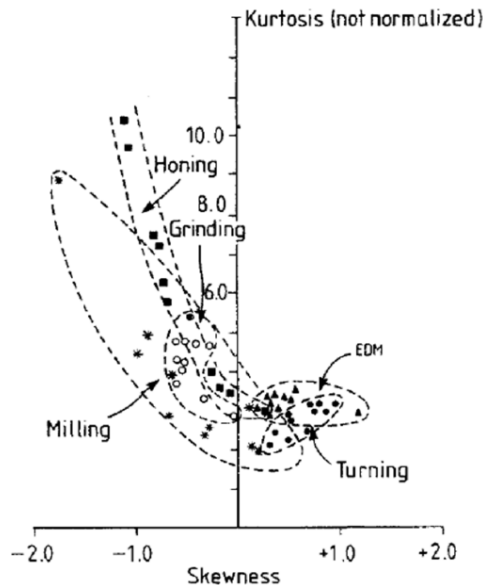


Fig. 1. The topological maps of surfaces made with different manufacturing technologies [18]

## 2. The materials and methods applied

### 2.1 The raw material and equipment used in the experiment

The most popular alloys for aluminium are silicon, copper and magnesium. One type of alloy (so-called AS17) widely used in industrial mass production were examined. The aluminum alloy examined combines excellent mechanical features with its technological advantages. The advantage of the AS17 (hyper-eutectic) material is its adequate hardness and wear resistance (due to primary silicon forming during the cooling process).

- raw material: AS17; composition:  $Al = 74.35\%$ ;  $Si = 20.03\%$ ;  $Cu = 4.57\%$ ;  $Fe = 1.06\%$  (further components:  $Pb, Sn, Ni, Ti (> 0.08\%)$ ; hardness:  $114 HB_{2.5/62.5/30}$ ; the size used in the cutting experiment:  $\varnothing 110 \times 40\text{ mm}$ ;
- the code of the toolholder: SDJCR 1616H 11;
- the code, material and geometry of the tools used: DCGW 11T304 FN, CVD-D, ISO and Wiper (see Fig. 2.);
- surface roughness tester: Mitutoyo SJ-301; the parameters of measurement:  $l = 4\text{ mm}$ ,  $\lambda_c = 0.8$ ,  $N = 5$ ; (The surface roughness on the workpiece was measured 12 times, every  $30^\circ$  degrees.);
- machine tool: EUROTURN 12B CNC lathe (The power of the spindle is  $P_{\max} = 7\text{ kW}$ , the maximum rpm is  $n_{\max} = 6000\text{ 1/min.}$ )

The presentation will be clear and concise and the symbols used therein will be specified in a symbol list (if necessary). In the paper it will be used the measurement units International System. In the paper, there will be no apparatus or installation descriptions.

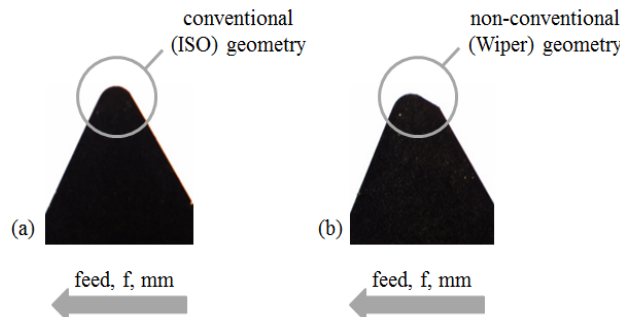


Fig. 2. Pictures of the tools used; (a) the tool of ISO geometry, code: DCGW 11T304 FN, edge materials: CVD-D (b) the tool of Wiper geometry, code: DCGW 11T304 FR-W, edge materials: CVD-D

## 2.2 The design of experiments applied

The experiments were carried out with the so-called central composite design whose settings can be seen in table 1. The investigated tools had conventional (ISO) and non-conventional (Wiper) edge geometry, therefore double feed was applied with the Wiper geometry tool [24].

Table 1

The experimental settings of the tools with different edge geometries

Experimental runs	cutting speed, $v_c$ , m/min	feed, $f$ , mm (ISO geometry)	feed, $f$ , mm (Wiper geometry)	depth of cut, $a$ , mm
1	667	0.058	0.116	0.267
2	667	0.058	0.116	0.733
3	667	0.112	0.224	0.267
4	667	0.112	0.224	0.733
5	1833	0.058	0.116	0.267
6	1833	0.058	0.116	0.733
7	1833	0.112	0.224	0.267
8	1833	0.112	0.224	0.733
9	500	0.085	0.17	0.5
10	2000	0.085	0.17	0.5
11	1250	0.05	0.1	0.5
12	1250	0.12	0.24	0.5
13	1250	0.085	0.17	0.2
14	1250	0.085	0.17	0.8
15 (C)	1250	0.085	0.17	0.5
16 (C)	1250	0.085	0.17	0.5

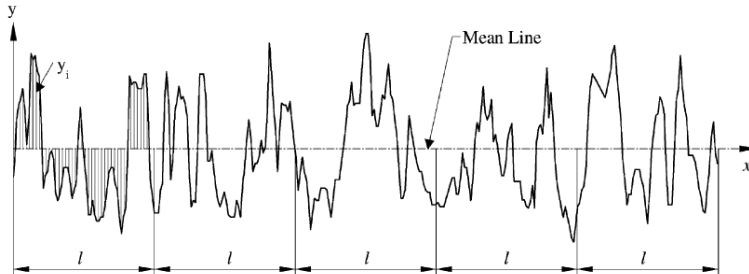
### 2.3 The surface roughness parameters examined

#### 2.3.1 Arithmetic average height ( $R_a$ )

This is one of the best-known surface roughness parameters (Fig. 3). It is the most often used characteristic in the industry because it is easy to measure and define. The mathematical definition and the digital implementation of the arithmetic average height parameter are as follows [25]:

$$R_a = \frac{1}{l} \int_0^l |y(x)| dx \quad (1)$$

$$R_a = \frac{1}{n} \sum_{i=1}^n |y_i| \quad (2)$$

Fig. 3. Specifying average height ( $R_a$ ) [25]

### 2.3.2 Root mean square roughness ( $Rq$ )

$Rq$  represents the standard deviation of the distribution of surface heights, so it is an important parameter to describe surface roughness with statistical methods. This parameter is more sensitive to large deviations from the mean line than the arithmetic average height ( $Ra$ ). The mathematical definition and the digital implementation of this parameter are as follows [25]:

$$Rq = \sqrt{\frac{1}{l} \int_0^l \{y(x)\}^2 dx} \quad (3)$$

$$Rq = \sqrt{\frac{1}{n} \sum_{i=1}^n y_i^2} \quad (4)$$

### 2.3.3 Ten-point height ( $Rz$ )

The ten-point height is more sensitive to extreme values (valleys, peaks) than  $Ra$ . The international ISO system defines this parameter as the difference in height between the average of the five highest peaks and the five lowest valleys along the assessment length of the profile. The German DIN system defines  $Rz$  as the average of the summation of the five highest peaks and the five lowest valleys along the assessment length of the profile. Fig. 4 shows the definition of the ten-point height parameter. The mathematical definitions of the two types of  $Rz$  are as follows [25]:

$$Rz_{(ISO)} = \frac{1}{n} \left( \sum_{i=1}^n p_i - \sum_{i=1}^n v_i \right) \quad (5)$$

$$Rz_{(DIN)} = \frac{1}{2n} \left( \sum_{i=1}^n p_i + \sum_{i=1}^n v_i \right) \quad (6)$$

where  $p_i$ s are the peak values, and  $v_i$ s are the valley values as can be seen in Fig. 4, and  $n$  is the number of samples along the assessment length.

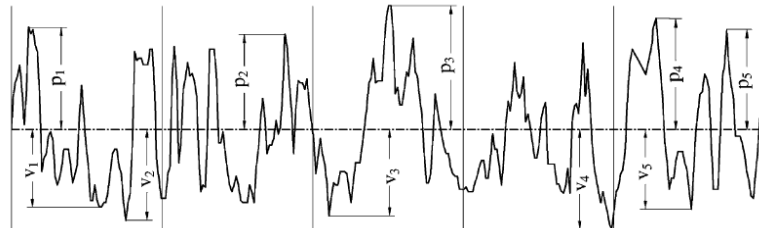


Fig. 4. Specifying ten-point height ( $Rz$ ) [25]

### 2.3.4 Maximum height of peaks ( $R_p$ )

$R_p$  is defined as the maximum height of the profile above the mean line within the assessment length as in Fig. 4.  $p_3$  represents the  $R_p$  parameter.

### 3.2.5 Maximum depth of valleys ( $R_v$ )

$R_v$  is defined as the maximum depth of the profile below the mean line within the assessment length as shown in Fig. 4. In Fig. 4.  $v_4$  represents the  $R_v$  parameter.

### 2.3.6 Skewness ( $R_{sk}$ )

The skewness of a profile is the third central moment of the profile amplitude probability density function, measured over the assessment length. This parameter is sensitive to occasional deep valleys or high peaks. A symmetrical height distribution, i.e. with as many peaks as valleys, has zero skewness. Profiles with peaks removed or deep scratches have negative skewness. Profiles with valleys filled in or high peaks have positive skewness. This is shown in Fig. 5.

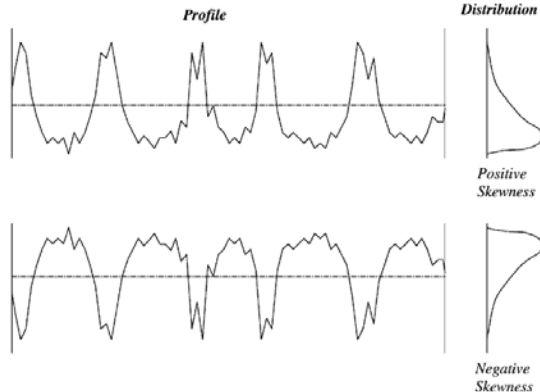


Fig. 5. Specifying skewness ( $R_{sk}$ ) [25]

The mathematical and numerical formula used to calculate the skewness of a profile, which has  $N$  points, are as follows [25]:

$$R_{sk} = \frac{1}{Rq^3} \int_{-\infty}^{\infty} y^3 p(y) dy \quad (7)$$

$$R_{sk} = \frac{1}{NRq^3} \left( \sum_{i=1}^n Y_i^3 \right) \quad (8)$$

where  $Y_i$  the height of profile at point number  $i$ .

### 2.3.7 Kurtosis ( $Rku$ )

The kurtosis coefficient is the fourth central moment of a profile amplitude. It describes the sharpness of the probability density of the profile. If  $Rku < 3$ , the distribution curve is said to be platykurtic and has relatively few high peaks and low valleys. If  $Rku > 3$  the distribution curve is said to be leptokurtic and has relatively many high peaks and low valleys. Fig. 6 shows these two types of kurtosis.

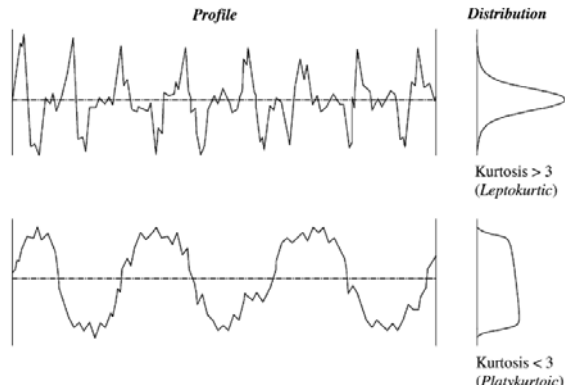


Fig. 6. Specifying kurtosis ( $Rku$ ) [25]

The mathematical and the numerical formula used to calculate the kurtosis of a profile are as follows [25]:

$$Rku = \frac{1}{Rq^4} \int_{-\infty}^{\infty} y^4 p(y) dy \quad (9)$$

$$Rku = \frac{1}{NRq^4} \left( \sum_{i=1}^n Y_i^4 \right) \quad (10)$$

## 3. Results

In the design of technology together with other parameters the roughness of the cut surface is an essential criterion. This chapter analyses the  $Ra$ ,  $Rz$ ,  $Rp$ ,  $Rv$ ,  $Rsk$  and  $Rku$  surface roughness values machined by the tools examined. The surface roughness values in the following diagrams are the average of 12 measurements.

### 3.1. The analysis of arithmetic average height ( $Ra$ ) and ten-point height ( $Rz$ )

Fig. 7 and 8 show  $Ra$  and  $Rz$  values plotted against the experimental runs. In the figures the values belonging to the two tools can be clearly seen. It can be

stated that lower surface roughness can be made with Wiper geometry tools, than with ISO geometry tools. The reason is that the edge part of the Wiper geometry in depth has a smaller end cutting edge angle than in case of ISO geometry. In this case the surface roughness parameters ( $R_a$ ,  $R_z$ ) are lower. As a result of this effect the high peaks disappear and the surface becomes finer.

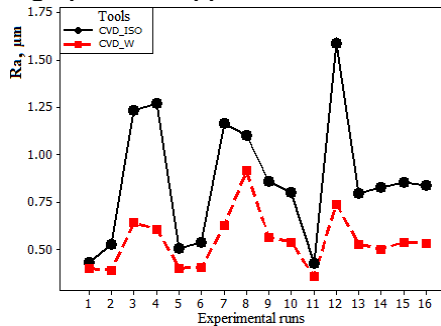


Fig. 7. The averages of  $R_a$  values plotted against the experimental runs

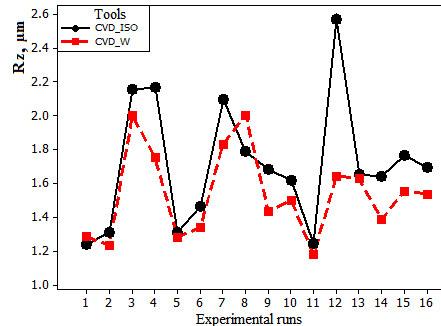


Fig. 8. The averages of  $R_z$  values plotted against the experimental runs

### 3.2. The analysis of maximum height of peaks ( $R_p$ ) and maximum depth of valleys ( $R_v$ )

Further important surface roughness values of the machined surface are  $R_p$  and  $R_v$ . The ratio of the two values characterizes the symmetry of the surface. If the value is around 1, the machined surface has a symmetrical profile. If the  $R_p/R_v$  ratio is higher than 1, the surface has high peaks, whereas if the ratio is lower than 1, a plateau surface profile is achieved. Fig. 9. shows these values for both tools examined.

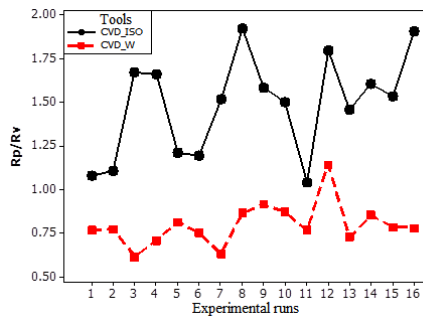


Fig. 9. The  $R_p/R_v$  ratio plotted against the experimental runs

This difference can be observed in the  $R_p/R_v$  ratio of surfaces machined by ISO and Wiper geometries. While in the case of ISO geometry tools the  $R_p/R_v$  ratio is between 1 and 2, the  $R_p/R_v$  ratio of Wiper geometry tools is below 1. The

above-mentioned differences between the  $Rp/Rv$  values are explained in Fig. 10 and Fig. 11.

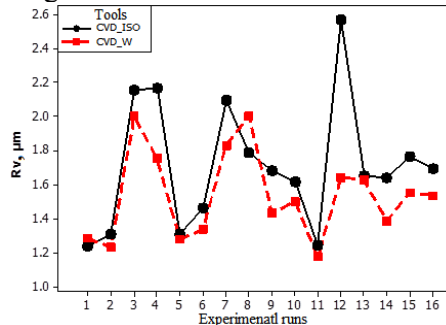


Fig. 10. The average of  $Rv$  values plotted against the experimental runs

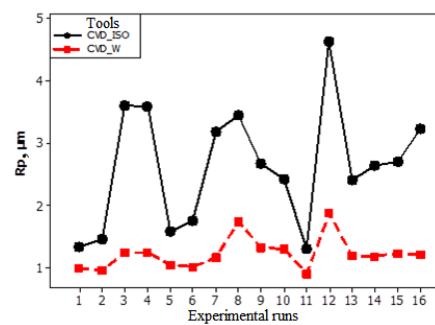


Fig. 11. The average of  $Rp$  values plotted against the experimental runs

In Fig. 10. the  $Rv$  values produced by the tools do not differ significantly. In Fig. 11. the  $Rp$  values of the machined surface can be seen. Here it is evident that the Wiper geometry tool manufactured significantly smaller  $Rp$  values in each experimental run therefore the differences in the  $Rp/Rv$  value depended mostly on the  $Rp$  values.

### 3.3. The analysis of the statistical parameters of surface roughness – topological map – ( $Rsk$ , $Rku$ )

The topological map represents kurtosis as a function of the skewness values of the different settings (in this case 16) on the  $Rsk$ ,  $Rku$  plane (see Fig. 1.). These two parameters influence to a great extent the expected working properties of the surface. Fig. 12. shows the topological map of the surfaces machined with the tools examined. In the topological map two groups of points can be observed, one for each tool geometry.

## 4. Conclusion

In this article the surface parameters ( $Ra$ ,  $Rz$ ,  $Rp$ ,  $Rv$ ,  $Rp/Rv$  ratio,  $Rsk$  and  $Rku$ ) of die-cast hyper-eutectic aluminium parts fine-turned with different edge geometry diamond tools were examined. The conclusion drawn from the results are the following:

- A relatively large amount of information can be obtained from a relatively small number of experimental runs with the use of the response surface method.
- The Wiper geometry tool produced significantly lower  $Ra$  and  $Rz$  values even at double feed. Therefore under the same criteria of surface parameters the

cutting time is half in this case than in case of ISO geometry tool, so the manufacturing costs can be also reduced.

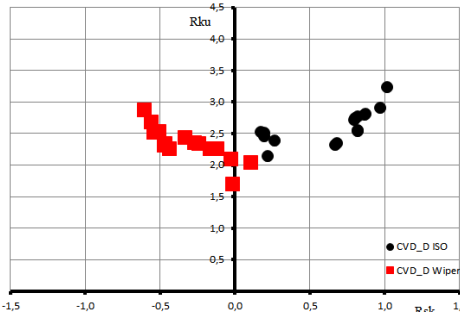


Fig. 12. The topological maps of the surfaces machined with the tools examined

- The  $Rp/Rv$  ratio, which characterizes the symmetry of surface roughness, is significantly lower in the case of surfaces machined with the Wiper geometry tool.

- It was proved that the reduction in the  $Rp/Rv$  ratio is due exclusively to the lower value of the  $Rp$  parameter – because of the “ironing effect” of the Wiper geometry – while the value of the  $Rv$  parameter is approximately the same in the case of both edge geometries.

- The  $Rsk$  and  $Rku$  parameters, which influence the load-bearing characteristics of the machined surface, negative skewness ( $Rsk$ ) with relatively high kurtosis ( $Rku$ ) – meaning better tribological performance – can be produced only with Wiper edge geometry.

## REFERENCE

- [1] G. N. Tóth, Á. Drégelyi-Kiss, B. Palásti-Kovács, Analysis of the microgeometric parameters of cut surfaces, Pollack Periodica: an international journal for engineering and information sciences **vol. 8**, 2013, pp. 55-66
- [2] Á. Drégelyi-Kiss, Á. Czifra, B. Palásti-Kovács, Comparison of capability calculations of surface roughness measurement in automotive industry, Proceedings of the ISMQC 2013., Cracow, Sept. 2013
- [3] B. Mikó, J. Beno, I. Mankova, Experimental verification of cusp heights when 3D milling rounded surfaces, Acta Polytechnica Hungarica **vol. 9**, 2012, no. 6, pp. 101-116
- [4] I. Sztankovics, J. Kundrák, Theoretical Value of Total Height of Profile in Rotational Turning. Applied Mechanics and Materials, **vol. 309**, 2013 pp. 154-161
- [5] Cs. Felhő, J. Kundrák, Comparison of Theoretical and Real Surface Roughness in Face Milling with Octogonal and Circural Inserts, Key Engineering Materials, **vol. 581**, 2014, pp. 360-365.
- [6] M. A. Dabnun, M. S. J. Hashmi, M.A. El-Baradie, Surface roughness prediction model by design of experiments for turning machinable glass-ceramic (Macor). Journal of Materials Processing Technology, 2005, pp. 1289–1293.
- [7] I. Maňková, M. Vrabel, J. Beňo, P. Kovac, M. Gostimirovic, Application of Taguchi Method and Surface Response Methodology to Evaluate Of Mathematical Models to Chip

Deformation when Drilling With Coated and Uncoated Twist Drills, Manufacturing Technology, **vol. 13**, 2013, no. 4, pp. 492-499

[8] J. Kundrák, Z. Pálmai, (2014). Application of general tool-life function under changing cutting conditions, Acta Polytechnica Hungarica **vol. 11**, 2014, no. 2, pp. 61-76

[9] J. P. Davim, Design of optimisation of cutting parameters for turning metal matrix composites based on the orthogonal arrays, Journal of Materials Processing Technology, 2003, pp. 340-344

[10] H. Aouici, M. A. Yallese, K. Chaoui, T. Mabrouki, J. F. Rigal, Analysis of surface roughness and cutting force components in hard turning with CBN tool: Prediction model and cutting conditions optimization, Measurement **vol. 45**, 2012, pp. 344-353

[11] B. Tukora, T. Szalay, Multi-dexel based material removal simulation and cutting force prediction with the use of general-purpose graphics processing units, Advances in Engineering Software **vol. 43**, 2012, pp. 65-70

[12] T. Szalay, F. Alpek, L. Monostori, S. Markos, Zs. Viharos, Investigation of machined surfaces using artificial intelligence methods, 9<sup>th</sup> International Conference on Tools, Miskolc, Hungary, 03 - 05 Sept. 1996, pp. 635-640

[13] T. Szalay, S. Markos, I. Mészáros, (1995). Monitoring of the cutting operations using fuzzy logic, 8<sup>th</sup> International Conference of AIEAE. Melbourne, Australia, 06 – 08 Juni. 1995, pp. 27-30

[14] R. Horváth, Á. Drégelyi-Kiss, Analysis of surface roughness parameters in aluminium fine turning with diamond tool, Measurement 2013 Conference, Smolenice, Slovakia, 13 May, 2013, pp. 275-278.

[15] R. Horváth, Á. Drégelyi-Kiss, Gy. Mátyási, Application of RSM method for the examination of diamond tools, Acta Polytechnica Hungarica, **vol. 11**, 2014, pp. 137-147

[16] R. Horváth, E. Tóth-Laufer, Fuzzy Model-Based Cutting Parameter Combination Optimization, Proc. of the 18<sup>th</sup> International Conference on Intelligent Engineering Systems (INES 2014), Tihany, Hungary, 03 – 05 July 2014, pp. 151-155

[17] R. Horváth, Gy. Mátyási, Á. Drégelyi-Kiss, Optimization of machining parameters for fine turning operations based on the response surface method, ANZIAM JOURNAL **vol. 55**, 2014, pp. C250-C265.

[18] D.J. Whitehouse, Handbook of surface metrology, Institute of Physics, Bristol, UK, 1994

[19] Á. Czifra, S. Horváth, Complex microtopography analysis in sliding friction of steel-ferodo material pair, Meccanica **vol. 46**, 2011, pp. 609-617

[20] W. Grzesik, K. Zak, Modification of surface finish produced by hard turning using superfinishing and burnishing operations, Journal of Materials Processing Technology, **vol. 212**, 2012, pp. 315– 322

[21] M. Sedlacek, B. Podgornik, J. Vizintin, Influence of surface preparation on roughness parameters, friction and wear, Wear, **vol. 266**, 2009, pp. 482–487

[22] P. L. Menezes, Kishore, S. V. Kailash, Influence of surface texture and roughness parameters on friction and transfer layer formation during sliding of aluminium pin on steel plate, Wear, **vol. 267**, 2009, pp. 1534–1549

[23] I. Barányi, The modification of the roughness parameters in the wear process, MECHEdu 2013, Serbia, Subotica Technical College of Applied Sciences, 2013 pp. 1-4

[24] W. Grzesik, T. Wanat, (2006). Surface finish generated in hard turning of quenched alloy steel parts using conventional and wiper ceramic inserts. International Journal of Machine Tools & Manufacture, **vol. 46**, 2006, pp. 1988–1995

[25] E.S. Gadelmawlaa, M.M. Kourab, T.M.A. Maksoucf, I.M. Elewaa, H.H. Solimand, Roughness parameters, Journal of Materials Processing Technology **vol. 123**, 2002, pp. 133-145